Effect of Tyrosine-Derived Triblock Copolymer Compositions on Nanosphere Self-Assembly and Drug Delivery

Larisa Sheihet, Karolina Piotrowska, Robert A. Dubin, Joachim Kohn, and David Devore*

New Jersey Center for Biomaterials, Rutgers, The State University of New Jersey, 145 Bevier Road, Piscataway, New Jersey 08854

Received September 8, 2006; Revised Manuscript Received November 1, 2006

We have obtained structure−activity relations for nanosphere drug delivery as a function of the chemical properties of a tunable family of self-assembling triblock copolymers. These block copolymers are synthesized with hydrophobic oligomers of a desaminotyrosyl tyrosine ester and diacid and hydrophilic poly(ethylene glycol). We have calculated the thermodynamic interaction parameters for the copolymers with anti-tumor drugs to provide an understanding of the drug binding by the nanospheres. We find that there is an optimum ester chain length, C8, for nanospheres in terms of their drug loading capacities. The nanospheres release the drugs under dialysis conditions, with release rates strongly influenced by solution pH. The nanospheres, which are themselves non-cytotoxic, deliver the hydrophobic drugs very effectively to tumor cells as measured by cell killing activity in vitro and thus offer the potential for effective parentarel in vivo delivery of many hydrophobic therapeutic agents.

Introduction

Self-assembling nanospheres offer a promising route to the delivery of pharmaceuticals that have poor bioavailability by improving the drugs' stability, circulation times in the body, and permeability through cell membranes, while reducing their toxicities.[1] Many drugs, including anti-tumor agents, antidepressants, and statins, are hydrophobic and therefore require a solubilization process to enable their parenteral delivery.[2] A variety of delivery strategies for these hydrophobic drugs has been explored, including polymeric and protein nanoparticles[3−6] and liposome vesicles.[7,8] Several of these are in clinical trials or have shown promise in preclinical evaluations.[6,9−11]

Of the many alternative approaches proposed to overcome the obstacle of poor bioavailability of the drug, perhaps the most promising is the use of amphiphilic block copolymers that self-assemble into supramolecular nanoparticles.[12] These nanoparticles can be designed to provide stable dispersions of hydrophobic drugs with low cytotoxicity, thus making them attractive alternatives to less mechanically stable liposomes or more cytotoxic surfactant dispersant systems such as the Cremophor EL, which has been associated with some of Taxol's serious clinical side effects.[13] The amphiphilic block copolymers typically form a core−shell architecture in which the hydrophobic core serves as the reservoir for the incorporation of liphophilic drugs and diagnostic agents[14] and the hydrophilic shell enables stable dispersion in an aqueous environment and frequently also offers protection from protein adsorption and subsequent biological attack.[15] Amphiphilic block copolymers with poly(ethylene glycol)[16] as the hydrophilic block and polyester,[17,18] poly(amino acid),[5,19,20] or polyether[21,22] as the hydrophobic block have been explored for applications in drug delivery. Particle size has been shown to be a critical design parameter, as particles with diameters less than 200 nm and having PEG shells avoid entrapment by the reticuloendothelial system (RES) and accumulate preferentially in tumors that typically exhibit an enhanced permeability and retention effect (EPR).[14,23] The biodistribution and uptake by the tumor of the nanoparticle is further dictated by charge density, conformation, hydrophobicity, and immunogenicity.[24,25] The drug loading efficiency of the nanoparticles is also governed by a number of critical parameters, particularly the chemical affinity of the loaded drug for the nanoparticle core.[26−28]

We have previously reported on the design and synthesis of symmetrical ABA-type amphiphilic triblock copolymers that self-assemble into nanospheres at low critical aggregation concentrations.[29,30] The A-blocks of these nanospheres are composed of poly(ethylene glycol) PEG, and the B-blocks are composed of oligomers of desaminotyrosyl-tyrosine alkyl esters (DTR) and nontoxic diacids. In addition to their biocompatibility, biodegradability, and lack of cellular toxicity, these nanospheres strongly bind the hydrophobic chemotherapeutic agent, paclitaxel. The nanospheres containing paclitaxel retain the anti-tumor cytotoxicity of free paclitaxel in vitro.[30] Here, we demonstrate the impact of the unique tunability of the tyrosine-based copolymers, which have four synthetically adjustable parameters, on the control of nanosphere architectures. Structure−activity relations are obtained for drug loading and delivery as a function of nanosphere architectures and drug hydrophobicity. We apply thermodynamic solubility parameter calculations for the interaction of the nanosphere hydrophobic blocks with drugs having a broad range of hydrophobicities to provide an understanding of the observed binding and release properties under dialysis conditions. Finally, we demonstrate that the nanospheres deliver the hydrophobic drugs very effectively to tumor cells in vitro.

Experimental Procedures

Special Note on Nomenclature. The abbreviation, DTR-XA/5K, is used to designate the various copolymer compositions in the family of ABA triblock copolymers. The PEG A-blocks are abbreviated as 5K, indicating the molecular weight and units of the PEG components (i.e., 5K = PEG5000). The oligo B-blocks are distinguished by both their alkyl pendent chain R linked to the DTR (desaminotyrosyl-tyrosine alkyl ester) unit and/or the diacid XA to form the DTR-ester (DTR-

* Corresponding author. Fax.: (732) 445-5006. E-mail: devore@biology.rutgers.edu.

10.1021/bm060860t CCC: $37.00
Published on Web 02/03/2007

Scheme 1. Structure of PEG-*b*-oligo(DTR-XA)-*b*-PEG Triblock Copolymers

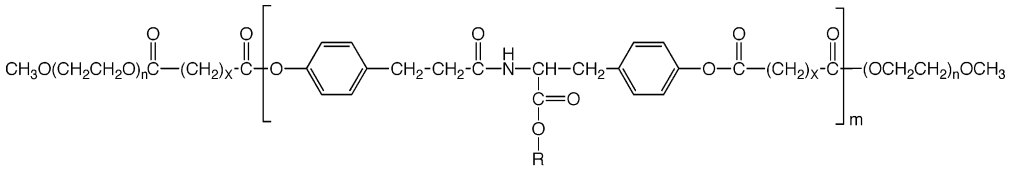

R = DTE (Ethyl, C2); DTO (Octyl, C8); DTD (Dodecyl, C12)
X = SA, Suberate (C6); DA, Dodecanoate (C10)

XA). The three pendent chains R used are (E) ethyl, (O) *n*-octyl, or (D) *n*-dodecyl, and the two diacids XA are (SA) suberic acid or (DA) dodecanodioic acid (Scheme 1). Therefore, DTO-SA/5K stands for the triblock copolymer PEG5K-*b*-oligo(desaminotyrosyl-tyrosine octyl ester suberate)-*b*-PEG5K. Other abbreviations are as follows: cytosine *b*-(D-arabinofuranoside free base), Ara C; camptothecin, CPT; and paclitaxel, PCL.

Materials. Methylene chloride (HPLC grade), methanol (HPLC grade), and 2-propanol were purchased from Fisher Scientific (Pittsburgh, PA). Suberic acid, dodecanedioic acid, 4-dimethylaminopyridinium-*p*-toluene sulfate (DMPTS), and poly(ethylene glycol) monomethyl ether (M_w 5000) were purchased from Aldrich Chemical Co. (Milwaukee, WI). Diisopropylcarbodiimide (DIPC) was purchased from Tanabe Chemicals (San Diego, CA). Dulbecco's phosphate buffered saline (pH 7.4), paclitaxel (from Taxus Yannanensis), camptothecin, and cytosine *b*-(D-arabinofuranoside free base) were purchased from Sigma (St. Louis, MO). *N*,*N*-Dimethylformamide (DMF) and tetrahydrofuran (THF) were obtained from Merck (EM Science, Darmstadt, Germany), and dimethyl sulfoxide (DMSO) was obtained from Merck and Sigma. All reagents were used as received.

Synthesis of PEG-*b*-oligo(DTR-XA)-*b*-PEG and Physical Characterization. The triblock copolymers were synthesized in a one-pot reaction at 20 °C using in situ carbodiimide coupling of the PEG and oligo(DTR-XA) as described elsewhere.[29,30] Reaction conditions such as monomer ratios, temperature, and reaction time were kept constant for all compositions. The chemical structure and purity of the triblock copolymers were confirmed by ^{1}H NMR (d_6-DMSO, Varian Unity 300 spectrophotometer, Palo Alto, CA). Molecular weights (M_n and M_w) were determined using gel permeation chromatography, GPC (PL-gel columns, pore size 10^5 and 10^4 Å, Perkin-Elmer, Shelton, CT; Waters 410 RI detector), with a 1 mL/min THF flow rate and polystyrene standards as M_w markers.

Nanosphere Preparation. Self-assembly of the polymers into nanospheres was induced by dropwise addition of 100 mg/mL of triblock copolymer in DMF solution into deionized water under mild agitation to a final copolymer concentration of 4 mg/mL. To remove particles greater than 220 nm in diameter, the resulting turbid aqueous dispersions were filtered through 0.22 μm low protein binding durapore syringe filters (PVDF, Millipore, Bedford, MA), and the filtrates were used for all subsequent characterizations. The hydrodynamic diameters of the nanospheres were obtained by dynamic light scattering at $q = 90°$, $\lambda = 523$ nm, and $T = 298$ K using cumulant fit analysis (Lexel argon ion laser; Fremont, CA) and a Brookhaven Instruments goniometer and correlator (BI-2030; Holtsville, NY). We refer to purified nanospheres as those that were processed as follows: the self-assembled nanosphere suspensions were filtered through 0.22 μm filters; the filtered nanospheres were isolated by ultracentrifugation of 12.25 mL nanosphere solutions at 65 000 rpm (290 000*g*) for 3 h at 25 °C (Beckman L8-70M ultracentrifuge, Beckman Coulter, Fullerton, CA), followed by removal of the supernatant; the pelleted nanospheres were then washed twice with water, resuspended with gentle agitation in 1 mL of water at 25 °C; the volume of the resuspended pellets was increased to 3 mL by the addition of water; and finally, the solutions were again filter sterilized (0.22 μm).

Nanosphere−Drug Interactions. Nanospheres with entrapped drugs were prepared by combining 60 mg of triblock copolymer with either 600 μg of Ara C, CPT, or PCL in 600 μL of DMF. These solutions were added dropwise to 14.4 mL of deionized water with constant stirring; the resulting suspensions were filtered (0.22 μm pore size), and purified drug containing nanospheres were obtained by ultracentrifugation and resuspension of the resultant pellet as described previously. To determine the maximum drug loading obtainable in the nanospheres, the initial drug feed concentration was increased while keeping all other parameters constant.

HPLC Assay. HPLC methods were developed and validated for quantitative determination of CPT, PCL, and Ara C in the copolymer systems. The concentrations of the drugs were assayed by high-performance liquid chromatography (HPLC) using a Waters 2695 HPLC system equipped with a UV/vis detector (Waters 2487, Dual l Absorbance Detector). Chromatographic separations were achieved using a RP-C18 column (Perkin-Elmer Brownlee Analytical C-18 column, 33 mm × 4.6 mm) at 25 °C. The mobile phase was a mixture of water (0.1% TFA)/acetonitrile (0.1% TFA) with a ratio of 75:25 (v/v), 55:45 (v/v), and 95:5 (v/v) for the assay of CPT, PCL, and Ara C, respectively. The mobile phase was delivered at a flow rate of 1 mL/min. The UV/vis detector was set at 370, 230, and 280 nm for CPT, PCL, and Ara C, respectively. Standard calibration samples were prepared at concentrations ranging from 2.5 to 75 μg/mL for all drugs. The calibration curves exhibited linear behavior over the concentration range of about 3 orders of magnitude. The detection limits were evaluated on the basis of a signal-to-noise ratio of 3 and were 0.02 μg/mL for CPT and 0.01 μg/mL for both PCL and Ara C. Within- and between-day precision and accuracy determinations of quality control samples were better than 10% across the range of the calibration curve. The specificity was determined by comparing the results obtained in the analysis placebo supernatant, containing only nanospheres, with those obtained in the analysis of all standard solutions of the drugs, and no interference from nanospheres was observed.

Drug Binding Efficiency. To determine the drug binding efficiency, a predetermined aliquot of the purified drug-loaded nanosphere suspension was withdrawn and freeze-dried, and the dry residue was weighed before dissolving in the extraction solvent. In the case of nanospheres containing CPT, lyophilized samples were dissolved in 1 mL of methylene chloride. CPT was extracted by the addition of 5 mL of 1 M NaOH to the organic phase followed by vigorous vortexing continued for 1 h. In the case of PCL containing nanospheres, lyophilized samples were dissolved in 5 mL of MeOH (extracting solvent) and vigorous vortexed for 1 h. A reversed phase high-performance liquid chromatography method developed for each drug was used to assay CPT in aqueous solution and PCL in organic solution, respectively. Drug entrapment by the nanospheres was characterized by two calculated ratios:

$$\text{binding efficiency (\%)} = \frac{\text{mass of drug in the nanosphere}}{\text{mass of drug in the feed}}$$

$$\text{loading efficiency (\%)} = \frac{\text{mass of drug in the nanosphere}}{\text{mass of nanospheres}}$$

In Vitro Drug Release. Release of CPT and PCL from drug loaded nanospheres was examined using a Slide-A-Lyzer dialysis diffusion technique (dialysis cassettes with a cutoff of 10 000 M_w CO, Pierce, Rockford, IL). A total of 2 mL of purified drug loaded nanosphere suspension was placed into preswelled dialysis cassettes and immersed

Table 1. Molecular Weight Properties of the PEG_{5K}-*b*-oligo(DTR-XA)-*b*-PEG_{5K} Triblock Copolymers and Their Corresponding Nanosphere Hydrodynamic Diameters

copolymer/ nanosphere composition	M_n	M_w	DP[a]	M_w/M_n	nanosphere hydrodynamic diameter (nm)[b]	poly-dispersity index[c]
DTE-SA/5K	20 000	25 000	19	1.25	122 ± 1.2	0.19
DTE-DA/5K	32 000	41 000	38	1.28	76 ± 1.4	0.22
DTO-SA/5K	23 000	29 000	21	1.26	55 ± 1.3	0.32
DTO-DA/5K	34 000	43 000	36	1.26	66 ± 1.6	0.28
DTD-SA/5K	23 000	29 000	19	1.26	72 ± 1.6	0.17
DTD-DA/5K	34 000	44 000	33	1.29	91 ± 1.5	0.18

[a] DP, degree of polymerization, was determined by the following equation: $(M_{n_{DTR\text{-}XA/5K}} - 2x(M_{n_{mPEG}}))/M_{w_{DTR\text{-}XA}}$. [b] Cumulant fit. The SD value was for the nanosphere mean hydrodynamic diameter obtained for the three measurements of a single batch. [c] Polydispersity $= \mu_2/\Gamma^2$, where $\mu_2 = (D^2 - D^{*2})q^4$ and $\Gamma = Dq^2$. D is the translational diffusion coefficient, D^* is the average diffusion coefficient, and q is the scattering vector.

in 150 mL of phosphate-buffered saline (PBS, 0.1 M) at pH 5.5, pH 7.4, or pH 10 at 37 °C with gentle agitation. Periodically, 10 mL of the external medium was withdrawn, and then 10 mL of fresh PBS of an appropriate pH was added to the system. The withdrawn sample solutions were freeze-dried and resuspended in 1 mL of water/methanol (1:1, v/v) for samples containing PCL or water/DMSO (1:1, v/v) for samples containing CPT and then analyzed by HPLC as described previously. All experiments were performed in duplicate.

In Vitro Biological Activity of Drug-Bounded Nanospheres. Biological activity of free drug and drug loaded nanospheres was determined using human KB tumor cells as previously described.[30] Briefly, serial dilutions of the free drug and purified nanosphere−drug suspension were added to the KB cells, and the cells were grown at 37 °/5% CO_2. Following 3 days of growth, the concentration required for 50% cell growth inhibition (LC50) was determined indirectly by an MTS assay following conditions described by the manufacturer. This assay was also used to compare the efficacy of drug entrapment and drug delivery by the nanospheres. The ratios of the LC50's of purified nanosphere solutions to filtered nanosphere solutions provided an estimate of the amount of drug effectively bound by the purified nanospheres. Comparisons of the LC50's of purified nanospheres to free (solvent solution) drug provided an indication of the effect of the nanospheres on drug activity.

Statistical Analysis. The results were analyzed statistically using the Student's *t*-test. When comparisons between groups yielded a value for $p < 0.05$, the difference between those groups was considered significant.

Results and Discussion

Nanosphere Size and Morphology. The chemical structure of the tyrosine-based triblock copolymers with varying pendent R chains and varying XA diacids is illustrated in Scheme 1. With a copolymer synthesis reaction time of 1 h, the copolymers are obtained with narrow molecular weight distributions centered around 25 kDA for all of the suberate (SA) esters and 44 kDA for all of the dodecanoate (DA) esters (Table 1). The copolymer molecular weights are not strongly affected by the pendent ester in the DTR monomers.

After self-assembly and purification, the block copolymer nanospheres have hydrodynamic diameters that go through a minimum size as the pendent ester chain lengths increase from ethyl (C4) to octyl (C8) to dodecyl (C12) (Table 1). This apparent minimum, which is reminiscent of the Ferguson effect for surfactant systems,[31] occurs for both the suberate and the dodecanoate esters at the same pendent octyl ester length. Given that the B-block chain lengths, as reflected by their degree of polymerization (DP), are very similar for all the suberates (DP ~20) and for all the dodecanoates (DP ~35), it can be concluded that the DTO nanospheres will have the most densely packed hydrophobic cores. The degree of polymerization was also measured by ^1H NMR, and very similar values were obtained (data not shown). The observed variations in self-organization behavior as a function of the DTR-XA core-forming blocks are consistent with their thermal properties.[32,33] Poly(DTE-XA)s are amorphous materials characterized by a glass transition, and they can be readily plasticized by water. In contrast, poly(DTD-XA)s possess long-range structural order with highly layered mesogenic properties, while poly(DTO-XA)s have less ordered structures typical in non-mesogenic macromolecules. An increase in the length of the core-forming block is expected to cause an increase in the core size of the nanospheres that, in turn, may result in an increased drug loading capacity per nanosphere.[26,34] With the exception that the DTE-SA/5K nanospheres are larger than the DTE-DA/5K nanospheres, the other nanospheres do follow this expected dependence on core block length. We believe the relatively large, unexpected size of DTE-SA/5K is due to its relatively weak hydrophobic core interactions and the core's relatively high affinity for water, which results in a more loosely packed architecture. Nevertheless, all of the copolymer formulations and their resultant nanospheres seem to be suitable for use in drug delivery based on their structural composition, polymer molecular weight distribution, and nanosphere size.

Table 2. Effect of Drug Hydrophobicity (log *D*) on In Vitro Drug Activity of Purified DTO-SA/5K Drug-Bounded Nanospheres

drug	mode of action	log *D*[a]	recovered activity (%)[b]
Ara C	DNA synthesis	−1.93	1 ± 0.3
Colchicine	microtubules	0.92	7 ± 2
Camptothecin	topoisomerase I	1.91	17 ± 8
Nocodazole	microtubules	2.43	54 ± 15
Rapamycin	immunophilin	3.58	56 ± 4
Paclitaxel	microtubules	3.62	44 ± 4

[a] pH 7; log *D* values were obtained from ACD/Labs (1994−2006 ACD/Labs). [b] Recovered drug activity (%) was recorded as a comparison between % growth inhibition activities of KB cells by initial (not purified) preparation of drug-bounded nanosphere and purified formulations. Data are expressed as ±SD for four independent measurements.

Nanosphere−Drug Compatibility and Binding Efficiency. The fraction of active drug entrapped in the purified DTO-SA/5K nanospheres increases as a function of the drug's hydrophobicity, as reflected in the drug's oil/water partition coefficient, log *D* (Table 2). Hydrophilic drugs such as Ara C (log $D = -1.93$) are not effectively entrapped by the nanospheres, while highly hydrophobic drugs like paclitaxel (log $D = 3.62$) are strongly bound by the nanospheres. The amount of biologically active drug entrapped by the purified nanospheres (i.e., drug that retains its anti-proliferative activity in in vitro KB tumor cell killing tests) is very close to the amount of bound drug obtained by HPLC analysis of the purified nanospheres (Figure 1). For example, the amount of biologically active paclitaxel entrapped by the DTO-SA/5K nanospheres is 44%, and the amount of chemically entrapped paclitaxel is 43%, which is indicative of extremely high efficiency of drug delivery to cells. Similarly, but at the other extreme, the fraction of unassociated Ara C is approximately 95% of the initial drug input based upon HPLC analysis, and the fraction of active drug is only 1% based upon the in vitro biological assay. Camptothecin exhibits a somewhat higher entrapment of 17% based on the

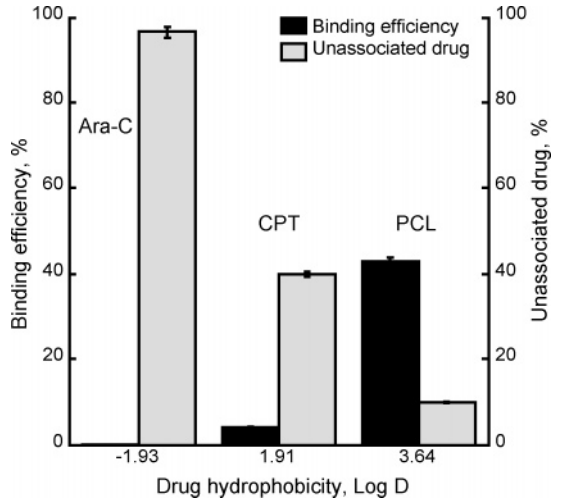

Figure 1. Effect of drug hydrophobicity on the binding efficiency of DTO-SA/5K nanospheres. Data expressed as ±SD of three independent measurements. Gray: drug recovered in supernatant using HPLC method and black: drug binding efficiency (wt %/wt) detected by extraction method and HPLC analysis.

biological assay than the 5% entrapment found by HPLC analysis. Despite its high log *D* value, camptothecin is poorly soluble in most organic solvents and has some tendency to self-aggregate. Hence, it is not surprising that it has low solubility in the hydrophobic DTO-SA block. On the other hand, the solubility of paclitaxel in the aqueous nanosphere suspensions is about 300-fold higher than the 0.25 mg/mL obtainable in water.

One of the most important factors dictating the extent of drug solubilization in the inner core of the nanospheres is the thermodynamic compatibility between the drug and the hydrophobic segments of the core. To assess this compatibility, we have applied Nagarajan's approach[26] by calculating the Flory–Huggins polymer–solute interaction parameters (χ_{SP})[35]

$$\chi_{SP} = \frac{(\delta_S - \delta_P)^2 V_S}{RT}$$

where χ_{SP} = interaction parameter between the solute (s) and the core-forming polymer block (p), δ_S = the Hoy solubility parameter of the solute, δ_P = the Hoy solubility parameter of the core-forming polymer block, and V_s = molar volume of the solute. The δ parameters were calculated for each B-block and the drugs PCL and CPT using Hoy's group contribution method.[36] Ideally, to achieve very high loading in the nanosphere carriers, the solubility parameters of the solute and the core-forming polymer should be the same (i.e., $\delta_S = \delta_P$, and hence, $\chi_{SP} = 0$).[27] The relatively low χ_{SP} values for PCL as compared to those for CPT are indicative of far greater compatibility of PCL with the tyrosine-based core blocks (Table 3). From these χ_{SP} values, it would be predicted that the DTE-SA/5K nanospheres would most effectively entrap CPT while the DTO-SA/5K nanospheres would be the optimum structure for binding PCL.

The experimentally observed bindings of CPT and PCL by the DTR-XA/5K nanospheres, obtained by HPLC analyses, are summarized in Figure 2. The binding of PCL is significantly greater than for CPT for all nanosphere compositions tested. The DTO containing nanospheres produce the maximum binding efficiency for both drugs regardless of the XA ester chain lengths. This is consistent with the optimum predicted by the χ_{SP} values for PCL but not for CPT. It can be concluded that

Table 3. Flory–Huggins Interaction Parameters (χ_{SP}) for Camptothecin and Paclitaxel Compatibility with Oligo(DTR-XA) Blocks

	δ_S ($J^{0.5}$ $cm^{-1.5}$)	δ_P ($J^{0.5}$ $cm^{-1.5}$)	χ_{SP} CPT	χ_{SP} PCL
CPT	23.22			
PCL	22.05			
DTE-SA		23.01	0.00	0.26
DTE-DA		22.42	0.06	0.04
DTO-SA		22.17	0.10	0.00
DTO-DA		21.76	0.20	0.02
DTD-SA		21.76	0.20	0.02
DTD-DA		21.42	0.30	0.11

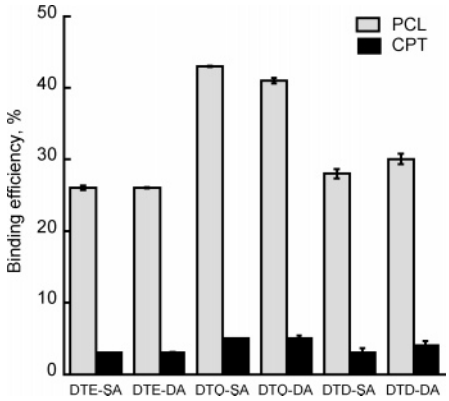

Figure 2. Drug binding efficiency as a function of hydrophobicity of the drug and hydrophobicity of the core-forming oligomers. Data expressed as ±SD of three independent measurements. Drug binding efficiency (wt %/wt) was detected by extraction method and HPLC analysis. (gray) PCL and (black) CPT.

the higher packing densities of the hydrophobic cores of the DTO nanospheres, as inferred previously from their smaller hydrodynamic diameters at equal chain lengths, have a very strong influence on the binding of the drugs. With shorter R groups, there can be greater water ingress and hence poorer solvency of the hydrophobic drugs, while at longer R groups (C10 and higher), there can be semicrystalline regions that would inhibit drug solubility.

Drug loading efficiency goes through a maximum as a function of the intial drug/copolymer feed ratio. The loading efficiency of DTO-SA nanospheres increases with increasing drug/copolymer feed ratios between 0.01 and 0.03 (wt/wt) and then decreases at higher feed ratios (Figure 3). Regardless of the feed ratio, the PCL loaded nanospheres appear stable in aqueous solution at each step of the purification procedure and retain a particle size of 55 nm, so disruption of the nanospheres does not appear to be the cause of the fall off in loading at the higher feed ratios. We believe that the fall off in loading is due to competitive equilibria between the drug and the nanosphere core and between the drug self-nucleation and the drug precipitation. This explanation is supported by visual observations of yellow precipitates of CPT at a feed ratio of 0.02 wt/wt for all copolymer nanosphere compositions. It is noted that the drug binding efficiency was measured following filtration through 0.22 μm filters, ultracentrifugation, and additional filtration through 0.22 μm filters for sterilization purposes. The initial filtration step strongly effects the drug binding efficiency because all nanosphere–drug particles and particles alone that are larger than 220 nm will be removed. It was found that this filtration step reduced the nanosphere yield as well as drug content in the nanospheres by 25% for paclitaxel-loaded nanospheres and 35% in camptothecin-bounded nanospheres

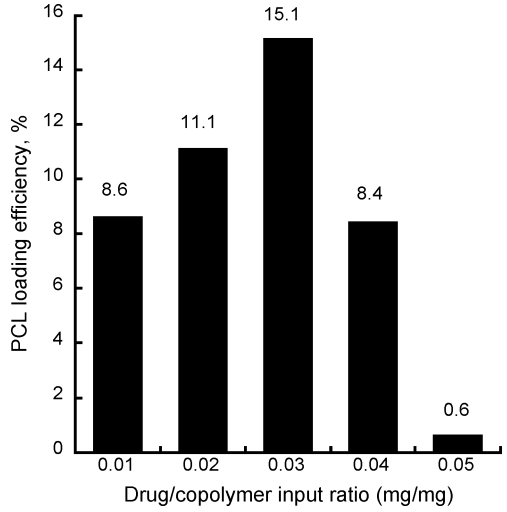

Figure 3. PCL loading efficiency (%) for DTO-SA/5K nanoparticles as a function of the drug/copolymer feed ratio. Copolymer concentration in the organic phase used for nanosphere preparation was fixed at 10 wt %/v. PCL was measured after solvent extraction using HPLC.

(data not shown). In spite of these loses, the PCL loading efficiency by DTO-SA/5K is about 15%, which is comparable to that of the commercially available PCL-loaded nanoparticle product, Abraxane.[37]

In Vitro Release of CPT and PCL. Dialysis equilibrium profiles of CPT and PCL from DTO-SA/5K nanospheres in phosphate buffered saline are indicative of an initial burst release of the drugs followed by a slow release phase (Figure 4). The initial burst release occurs within the first few hours of incubation and may be attributable to drug molecules associated with the interface of the nanosphere hydrophobic core and PEG corona, while the slow release process depends on the diffusion of drug from the nanosphere core region. The burst release of CPT amounts to 70% of the total bound drug in 5 h, as compared to 25% of the total bound PCL released in the same amount of time. The faster release of CPT as compared to PCL can be attributed to the lower initial loading of CPT in the nanospheres and the higher aqueous solubility (lower log D) of CPT.[28] We have previously reported on the high, extended stability of our nanospheres under physiological conditions for several months and also their very low critical aggregation concentrations.[29,30] Nanosphere dissociation and degradation is therefore not a significant factor in the observed drug release profiles. The relatively fast release kinetics of both drugs can, however, be attributed to the low T_g (21 °C) of the hydrophobic copolymer core.[30] The low T_g is indicative of a mobile polymeric matrix that enables rapid diffusion of small drug molecules.[27]

The release kinetics of both PCL and CPT are strongly dependent upon the pH of the outer dialysis solutions; the lower the pH, the faster the release (Figure 4). After 72 h, 100% of CPT is released at pH 5.5 as compared to just 84% at pH 7.4 and only 60% at pH 10. For PCL, the release rates are substantially less than for CPT at all times. At 72 h, the release of PCL is 72% at pH 5.5 and only 20% at pH 10. The measured hydrodynamic diameters of PCL containing nanospheres recovered from the dialysis cassettes after 72 h of dialysis at pH 5.5, 7.4, and 10 are 53 ± 1.2, 54 ± 1.3, and 43 ± 0.9 nm, respectively. Thus, the higher release rate at pH 5.5 than pH 10 was not due to the destruction of the nanospheres. The pH dependence of the drug release profiles is expected to have an important therapeutic advantage in that the drugs will be bound to the nanospheres at pH 7.4, which is typical of the blood

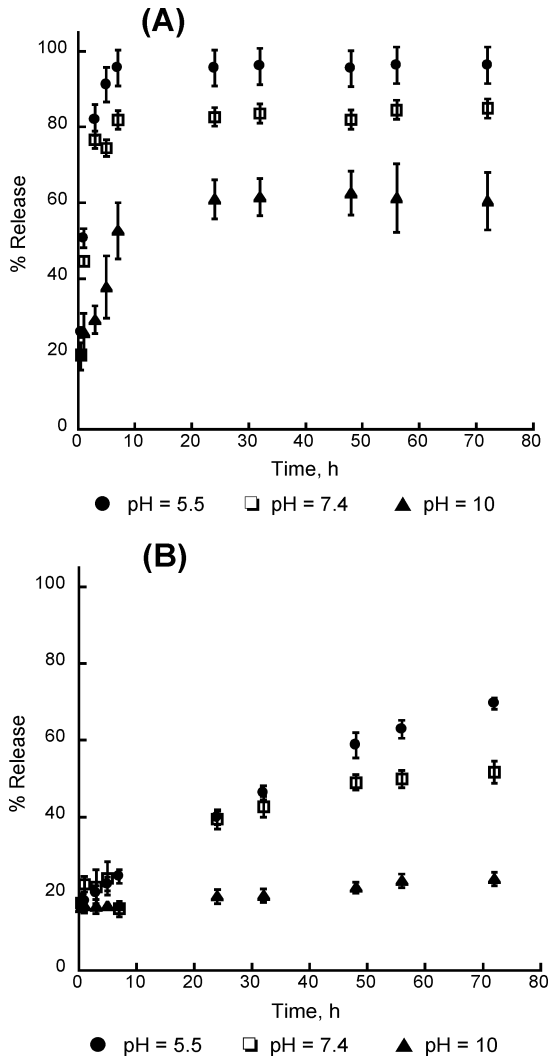

Figure 4. Release profiles of CPT (A) and PCL (B) loaded DTO-SA/5K nanospheres in different pH media at 37 °C.

stream, but drug release will be enhanced at pH 5.5, which is typical of the intracellular environment.

Nanosphere−Drug Activity. The LC50 values in KB human carcinoma cell in vitro are 24.7 ± 4.6 ng/mL for free PCL and 4.2 ± 0.1 ng/mL for PCL in DTO-SA/5K nanospheres. Similarly, LC50 values of 95 ± 18 and 62 ± 14 ng/mL are obtained for free CPT and CPT in DTO-SA/5K, respectively. Thus, for both drugs, the nanospheres provide substantially enhanced drug delivery. In these experiments, the KB cells are treated with the same concentrations of the drugs and analyzed by MTS colorimetric assays for cell viability after 3 days. As previously reported, DTO-SA/5K nanospheres alone do not display cytotoxicity under the same experimental conditions.[30] Hence, these nanospheres are excellent candidates for in vivo delivery of hydrophobic drugs for cancer chemotherapy and many other therapeutic applications.

Conclusion

The chemical composition of the tyrosine-based triblock copolymers has a profound effect upon the size of the self-assembled nanospheres obtained from these copolymers and upon the drug binding properties of these nanospheres. For the anti-tumor drugs investigated herein, it is found that there is an optimum degree of hydrophobic properties in the copolymers

that is attained with the octyl ester of the oligo(DTR-XA) hydrophobic block. The extent of drug loading is strongly influenced by the thermodynamic solubility parameters of the drugs and copolymer blocks, as well as by the packing density and mobility of the hydrophobic block chains within the nanosphere core, which is in general accord with the available theory. The nanospheres release bound drugs rapidly under physiological conditions, and the release rates are dependent upon the drug loading properties of the nanospheres and the pH of the solution. The nanospheres provide highly effective delivery of the hydrophobic anti-tumor drugs PCL and CPT to human tumor cells in vitro and thus offer the potential for parenteral delivery of a wide array of hydrophobic drugs in vivo without the cytotoxicity problems commonly exhibited by surfactant-based drug delivery systems. Preclinical studies on the anti-cancer activities of novel paclitaxel containing tyrosine-derived nanospheres are ongoing and to be reported in the near future.

Acknowledgment. The authors thank Dr. Paul Holmes (New Jersey Center for Biomaterials) for useful discussions and insight and Prof. Robert Prud'homme (Princeton University) for use of the light scattering instrument. Support for this work from the New Jersey Center for Biomaterials and Center for Military Biomaterials Research Grant W81XWH-04-2-0031 is acknowledged.

References and Notes

(1) Myrdal, P. B.; Yalkowasky, S. H.; Swarbick, J.; Boylan, J. C. *Encyclopedia of Pharmaceutical Technology*; Marcel Dekker: New York, 2002.
(2) Gelderblom, H.; Verweij, J.; Nooter, K.; Sparreboom, A. *Eur. J. Cancer* **2001**, *37*, 1590−1598.
(3) Potineni, A.; Lynn, D. M.; Langer, R.; Amiji, M. M. *J. Controlled Release* **2003**, *86*, 223−234.
(4) Opanasopit, P.; Yokoyama, M.; Watanabe, M.; Kawano, K.; Maitani, Y.; Okano, T. *Pharm. Res.* **2004**, *21*, 2001−2008.
(5) Yokoyama, M.; Opanasopit, P.; Okano, T.; Kawano, K.; Maitani, Y. *J. Drug Target* **2004**, *12*, 373−384.
(6) Gradishar, W. J.; Tjulandin, S.; Davidson, N.; Shaw, H.; Desai, N.; Bhar, P.; Hawkins, M.; O'Shaughnessy, J. *J. Clin. Oncol.* **2005**, *23*, 7794−7803.
(7) Torchilin, V. P. *Adv. Drug Delivery Rev.* **2005**, *57*, 95−109.
(8) Williams, J.; Lansdown, R.; Sweitzer, R.; Romanowski, M.; LaBell, R.; Ramaswami, R.; Unger, E. *J Controlled Release* **2003**, *91*, 167−172.
(9) Kim, T. Y.; Kim, D. W.; Chung, J. Y.; Shin, S. G.; Kim, S. C.; Heo, D. S.; Kim, N. K.; Bang, Y. *J. Clin. Cancer Res.* **2004**, *10*, 3708−3716.
(10) Matsumura, Y.; Hamaguchi, T.; Ura, T.; Muro, K.; Yamada, Y.; Shimada, Y.; Shirao, K.; Okusaka, T.; Ueno, H.; Ikeda, M.; Watanabe, N. *Br. J. Cancer* **2004**, *91*, 1775−1781.
(11) Danson, S.; Ferry, D.; Alakhov, V.; Margison, J.; Kerr, D.; Jowle, D.; Brampton, M.; Halbert, G.; Ranson, M. *Br. J. Cancer* **2004**, *90*, 2085−2091.
(12) Zhang, L.; Eisenberg, A. *Polym. Adv. Technol.* **1998**, *9*, 677−699.
(13) Dorr, R. T. *Ann. Pharmacother.* **1994**, *28*, 11−14.
(14) Torchilin, V. P. *J. Controlled Release* **2001**, *73*, 137−172.
(15) Haag, R. *Angew. Chem., Int. Ed.* **2004**, *43*, 278−282.
(16) Greenwald, R. B.; Choe, Y. H.; McGuire, J.; Conover, C. D. *Adv. Drug Delivery Rev.* **2003**, *55*, 217−250.
(17) Allen, C.; Han, J.; Yu, Y.; Maysinger, D.; Eisenberg, A. *J. Controlled Release* **2000**, *63*, 275−286.
(18) Liggins, R. T.; D'Amours, S.; Demetrick, J. S.; Machan, L. S.; Burt, H. M. *Biomaterials* **2000**, *21*, 1959−1969.
(19) Shenoy, D.; Little, S.; Langer, R.; Amiji, M. *Pharm. Res.* **2005**, *22*, 2107−2114.
(20) Kataoka, K.; Matsumoto, T.; Yokoyama, M.; Okano, T.; Sakurai, Y.; Fukushima, S.; Okamoto, K.; Kwon, G. S. *J. Controlled Release* **2000**, *64*, 143−153.
(21) Kabanov, A. V.; Batrakova, E. V.; Alakhov, V. Y. *Adv. Drug Deliv. Rev.* **2002**, *54*, 759−779.
(22) Batrakova, E. V.; Li, S.; Miller, D. W.; Kabanov, A. V. *Pharm. Res.* **1999**, *16*, 1366−1372.
(23) Xu, Z. K.; Nie, F. Q.; Qu, C.; Wan, L. S.; Wu, J.; Yao, K. *Biomaterials* **2005**, *26*, 589−598.
(24) Haag, R.; Kratz, F. *Angew. Chem., Int. Ed.* **2006**, *45*, 1198−1215.
(25) Maeda, H.; Sawa, T.; Konno, T. *J. Controlled Release* **2001**, *74*, 47−61.
(26) Nagarajan, R.; Ganesh, K. *Macromolecules* **1989**, *22*, 4312−4325.
(27) Allen, C.; Maysinger, D.; Eisenberg, A. *Colloids Surf., B* **1999**, *16*, 3−27.
(28) Soo, P. L.; Luo, L.; Maysinger, D.; Eisenberg, A. *Langmuir* **2002**, *18*, 9996−10004.
(29) Nardin, C.; Bolikal, D.; Kohn, J. *Langmuir* **2004**, *20*, 11721−11725.
(30) Sheihet, L.; Dubin, R. A.; Devore, D.; Kohn, J. *Biomacromolecules* **2005**, *6*, 2726−2731.
(31) Morrison, I. D.; Ross, S. *Colloidal Dispersions: Suspensions, Emulsions, and Foams*; John Wiley and Sons, Inc.: New York, 2002.
(32) Jaffe, M.; Ophir, Z.; Collins, G.; Recber, A.; Yoo, S.-u.; Rafalko, J. *Polymer* **2003**, *44*, 6033−6042.
(33) Jaffe, M.; Pai, V.; Ophir, Z.; Wu, J.; Kohn, J. *Polym. Adv. Technol.* **2002**, *13*, 926−937.
(34) Gadelle, F.; Koros, W. J.; Schechter, R. S. *Macromolecules* **1995**, *28*, 4883−4892.
(35) Nagarajan, R.; Maureen, B.; Ruckensteinf, E. *Langmuir* **1986**, *2*, 210−215.
(36) Van Krevelen, D. W. *Properties of Polymers*; Elsevier Science B.V.: Amsterdam, The Netherlands, 1997.
(37) Desai, N.; Trieu, V.; Yao, Z.; Louie, L.; Ci, S.; Yang, A.; Tao, C.; De, T.; Beals, B.; Dykes, D.; Noker, P.; Yao, R.; Labao, E.; Hawkins, M.; Soon-Shiong, P. *Clin. Cancer Res.* **2006**, *12*, 1317−1324. Abraxis Oncology. *Abraxane for Injectable Suspensions*; Schaumburg, IL, 2005; insert 451031.

BM060860T